

# Design of a High-Performance Composite Triple Clamp of Motorbike



Akshay B, Sony Alias, Ramesh Kumar R

**Abstract:** A simple and novel design concept for a CFRP composite triple clamp of a motorbike is brought out for low mass that fulfills the stiffness and strength requirement when compared to an existing steel triple clamp. In general, for any triple clamp configuration, the ideal fibre angle is chosen as the angle that subtends in the arm of the clamp with respect to the longitudinal direction (a line connecting the two fork holes). The initial design configuration is fabricated using a commercially available low modulus bi-directional carbon-epoxy laminate and tested for the evaluation of axial and transverse stiffnesses. Finite element model is then verified through the test data. Using the validated FE model, a new design with the high modulus carbon-fiber is arrived at. The proposed composite design suitable for high performance motorbike that possesses, high margin over critical load case with low mass when compared to steel clamp is provided.

**Keywords :** Fiber Stress, Composite element, Motorbike, Twist Load.

## I. INTRODUCTION

High performance (400 cc and above) bikes tend to be heavier with the use of steel or aluminum alloy and hence put a large force on the front suspension system (Fig. 1). This demands high structural capabilities in terms of strength and stiffness. The design demand in these bikes is met by increasing the size of the triple clamp which makes them heavier. A heavy bike is always difficult to maneuver. Making the bikes lighter is always a challenge in motorsport. Thus, the company has to compromise between structural performance and weight while designing a triple clamp.

Triple clamp is one of the structural components of a motorbike which connects the chassis to the front forks (Fig. 1-2). The triple clamp has an upper clamp, a lower clamp and a stem connecting the two. The lower clamp is closer to the front tire and takes different types of forces acting on the front tire like the braking force and the normal reaction from the road. In 1982 Odom and Adams [1]

designed a carbon-fiber swing-arm to meet the strength and stiffness criteria. Similar study by Eugenio et. al. and Airoldi et. al. for a composite swing-arm were also reported with 50% reduction in mass [2-3].

As of today, no composite triple clamp design is reported in literature. Laminate configuration with the use of high strength and stiffness carbon-epoxy laminate is envisaged in

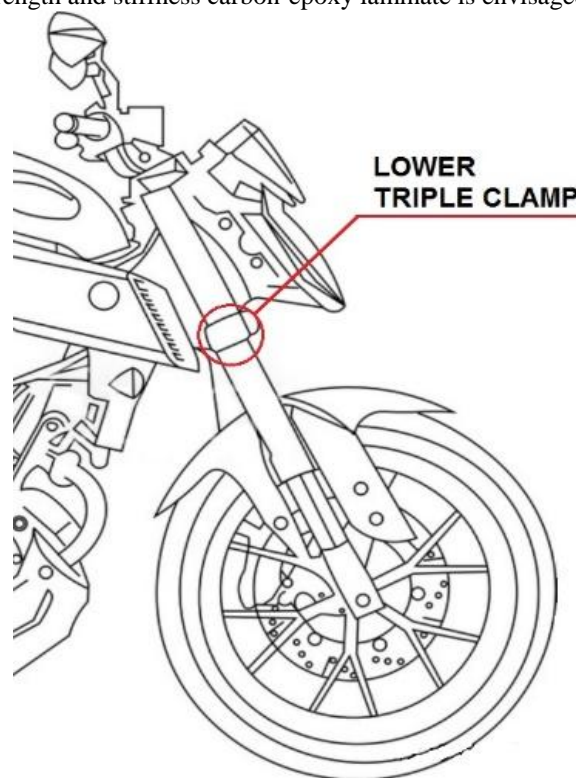


Fig.1. Triple Clamp in a Motorbike

Revised Manuscript Received on January 30, 2020.

\* Correspondence Author

**Akshay B\***, Department of Mechanical Engineering, College of Engineering Trivandrum, India. Email: akshyabtacha@gmail.com

**Sony Alias**, Department of Mechanical Engineering, College of Engineering Trivandrum, India. Email: sonyalias97@gmail.com

**Ramesh Kumar R**, Department of Mechanical Engineering, Sree Chitra Thirunal College of Engineering, Trivandrum, India. Email: rameshkumar9446@gmail.com

© The Authors. Published by Blue Eyes Intelligence Engineering and Sciences Publication (BEIESP). This is an open access article under the CC-BY-NC-ND license <http://creativecommons.org/licenses/by-nc-nd/4.0/>

## Design of a High-Performance Composite Triple Clamp of Motorbike

the present study to further lighten the clamp (Table I). In this work a novel approach is followed for the design of a composite lower triple clamp to reduce the mass when compared to an existing steel clamp.

Initially for an available low modulus carbon fabric, the clamp is fabricated and tested. Finite element model is then verified through the test data. The design of the composite triple clamp with high modulus material is analyzed and compared with steel clamp and the efficacy of the design is brought out.

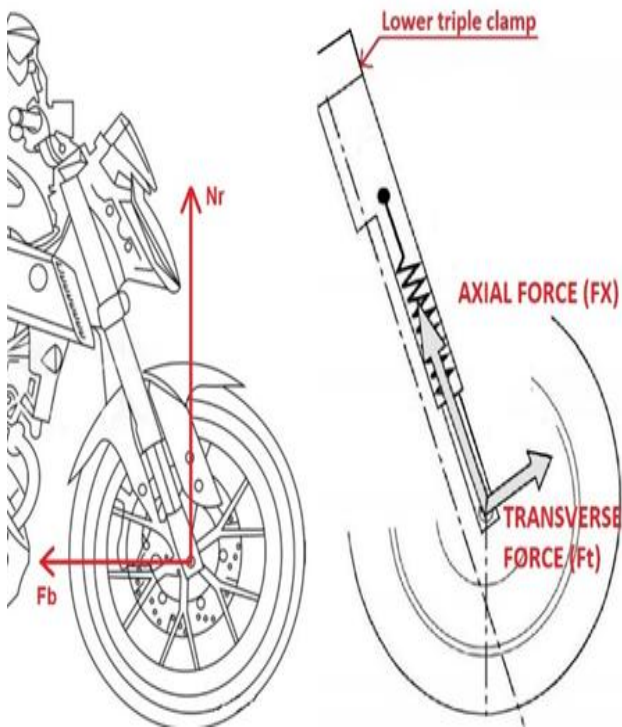


Fig. 2. Forces acting on the front suspension system

## II. DESIGN SPECIFICATION OF TRIPLE CLAMP

### A. Loads

From Fig. 2, it can be seen that the forces acting on the front tires of the motorbike are conveyed to the chassis through the triple clamp. The major forces acting on the front tire are as follow:

- (i) Braking force ( $F_b$ )
- (ii) Normal reaction ( $N_r$ ) exerted by the road

The forces  $F_b$  and  $N_r$  can be resolved into 2 mutually perpendicular forces as shown in the Fig. 2. There is the axial force ( $F_x$ ) which acts along the forks and the transverse force ( $F_t$ ) which acts perpendicular to the forks. The direction of  $F_x$  can be assumed to be in the upward direction.  $F_t$  reverses its direction depending on whether the bike is running freely or being braked. On transferring the loads from the wheel pin to the lower clamp, in addition to  $F_x$  and  $F_t$ , a moment  $M$  is also to be considered (Fig. 3), where

$$M = Ft \times 0.5 \quad (1)$$

Here, 0.5 m is the distance from the wheel pin to the lower clamp. Although the load from the forks is shared by upper and lower clamps (Fig. 1), in the design however, the lower

clamp is assumed to take the entire load which makes the design more conservative. It may be noted that  $M$  reverses its sign as  $F_t$  reverses.

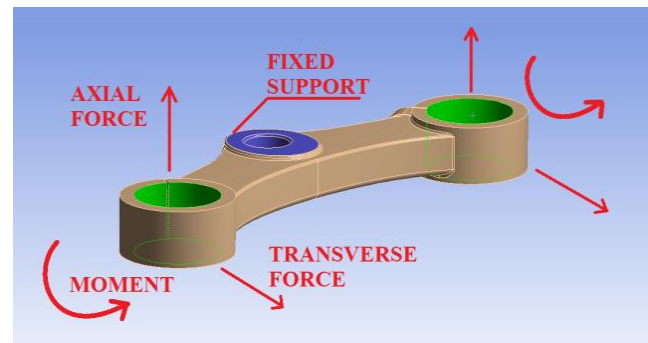


Fig. 3. Free body diagram of lower triple clamp

### B. Performance Requirements and Assessment

$F_x$ ,  $F_t$  and  $M$  are the major types of loads acting on the triple clamp. The performance of the clamp is dictated by failure load and stiffness of the clamp. In the present study these values correspond to that of metallic clamp. This necessitates the definition of 3 types of stiffness and associated strengths that are axial stiffness ( $K_x$ ), transverse stiffness ( $K_t$ ) and twist stiffness ( $K_\theta$ ), axial failure load ( $F_{xu}$ ), transverse failure load ( $F_{tu}$ ) and twist failure load ( $M_u$ ). The stiffness values  $K_x$  and  $K_t$  are calculated by measuring the force required for unit displacement of the nodes on a reference line (Fig. 4). The value of  $K_\theta$  is found by measuring the moment required to rotate the reference line by unit degree. The failure load is arrived at based on the analysis.

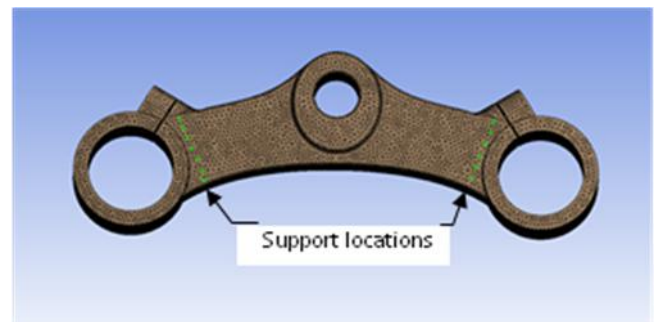


Fig. 4. Constrained nodes on the reference line of metallic clamp model

### C. Geometry and Material Properties of Triple Clamp

For the present work, a steel triple clamp of Dominar 400 (Fig. 5(a)) is taken as the reference design [4]. The critical dimensions of the composite clamp are shown in Fig. 5 (b). The material properties of steel composite triple clamp are given in Table I. The composite design is realized using a commercially available low modulus bi-directional carbon fabric, the modulus of which is found experimentally by the three-point bend test. For the actual design, high modulus carbon-epoxy laminate is considered.

Table- I: Properties considered for triple clamp

	Steel AISI 4340 [5]	High modulus carbon–epoxy laminate, M55J/M18 [6]
Longitudinal Young’s Modulus	200 GPa	300 GPa
Transverse Young’s Modulus	200 GPa	6 GPa
Major Poisson ratio	0.3	0.34
Yield Strength	1185 MPa	-----
Tensile Strength, X <sub>T</sub>	-----	1600 MPa
In-plane shear modulus	-----	4.5 GPa
Density	7.85 g/cm <sup>3</sup>	1.6 g/cm <sup>3</sup>

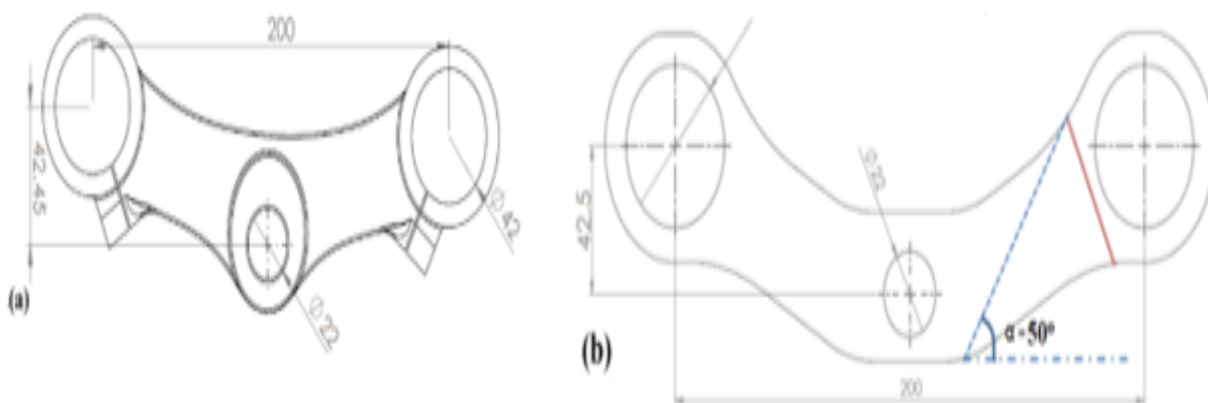


Fig. 5. Comparison of geometries of (a) metallic and (b) composite triple clamp (not to scale)

### III. METHODOLOGY

The performance characteristics of the steel design is used as the benchmark for comparison of the new composite design.

Step 1: Low modulus bi-directional carbon-epoxy triple clamp is fabricated with 57 number of layers of zero-degree plies (each 0.42 mm) to obtain the product as shown in the Fig. 6(a) and Fig. 7.

Step 2: Three-point bend test of coupon (bi-directional) from the composite slab used for the clamp is carried out to obtain the flexural modulus (Fig. 6(b)) [7]. Poisson’s ratio and shear modulus are taken from Table 1.

Step 3: FE model is validated based on comparison of the test data on stiffness with analysis (Fig. 6(c-d)).

Step 4: Analysis is repeated for the stiffness evaluation of composite clamp using high modulus material.

Step 5: Analysis for steel configuration is also studied for the estimation of K<sub>x</sub>, K<sub>t</sub> and K<sub>θ</sub> (vide Sec. II.B). Then failure loads based on von Mises criterion is arrived at

Step 6: Stiffness of the composite clamp is compared with the existing steel design.

### IV. DESIGN OF COMPOSITE TRIPLE CLAMP

The preliminary design of the clamp is envisaged with a lay-up sequence of (0<sub>2</sub>/±α)<sub>s</sub> to achieve stiffness. In order to enhance transverse and twist stiffness, α is arrived at as shown in Fig. 5(b) and α is measured as 50 degrees. Since the

thickness of the steel clamp is around 20 mm, the following lay-up sequence is considered. Thus,

The possible optimum lay-up Sequence becomes (0<sub>2</sub>/±50)<sub>30</sub> (0.1 mm Ply Thickness) for the high modulus carbon epoxy laminate (vide – Table I)



**Fig. 6. Experimental set up for evaluation for data generation to validate FE model**

### V. EXPERIMENTAL EVALUATION OF STIFFNESS

A commercially available plain-weave bidirectional carbon fabric of 0.42 mm dry thickness is chosen for the initial design. A composite slab of dimensions 125 mm x 294 mm x 24 mm is designed, out of which the required composite clamp profile is then cut out. The sectional dimensions of the arms of the clamp are decided to be 35 mm x 24 mm. For a thickness of 24 mm, 57 plies are stacked up with 0° orientation (w.r.t global x-axis) as shown in the Fig. 7. Epoxy resin is applied over each ply. The composite slab is then vacuum bagged and cured at room temperature. The composite clamp profile is then cut from the slab using water jet. Then vacuum bagging is repeated for providing two layers of hoop wrapping to each arm of the clamp to avoid any possible delamination.

#### A. Three Point Bend Test

The three-point bend test is done to evaluate the flexural modulus of coupon as well as the stiffness of the clamp. A cuboidal coupon of 23 x 12 x 150 mm is cut from the composite slab and tested (Fig. 6(b)). The composite triple clamp is placed in appropriate orientation to measure the axial and transverse stiffness (Fig. 6(c-d)).

### VI. FINITE ELEMENT ANALYSIS

Composite triple clamp for the low modulus fabric is modeled using four node quadrilateral and triangular elements with six degrees of freedom to accommodate the shape (Fig. 7). Global coordinate system is followed with respect to zero-degree plies. For the performance estimation of the redesigned high modulus clamp, the same FE model is

used with proper fiber orientations for each layer for laminate sequence of  $(0_2/\pm 50)_{30}S$  (0.1 mm ply thickness). Analyses are carried out for five types of loading, two for finite element model validation using low modulus laminate (Fig. 6(c-d)) and three for performance estimation for the high modulus carbon -epoxy laminate (Fig. 8(a-c)), Table I).

#### A. Type of Loading for Evaluation of Axial Stiffness (Low Modulus)

For finite element model validation, load and boundary conditions are given similar to the test case. The loading pin is modeled using brick element elements and coupled with the contact interface with the only degree of along the loading direction (Fig. 7). Nodes along the width of the arm close to fork hole on either side as indicated by dotted lines in Fig. 4 are given simply supported boundary conditions.

#### B. Type of Loading for Evaluation of Transverse Stiffness (Low Modulus)

Similar boundary conditions across the thickness at the support locations are shown in Fig. 6(d).

#### C. Type of Loading for Evaluation of Axial Stiffness (High Modulus)

For the final design of triple clamp, stiffnesses are evaluated only through analysis. Fig. 8(a) shows the axial loading acting at the center of fork holes. All nodes on the periphery of the fork hole are coupled to the center node on which the axial load is applied. A typical load of 1000N is given. All nodes close to the central stem (Fig. 1) are fully

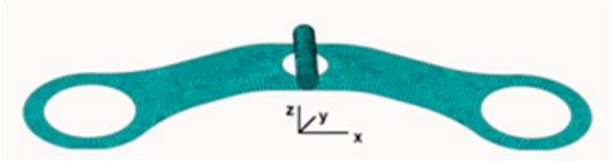


Fig. 7. FE model of composite clamp

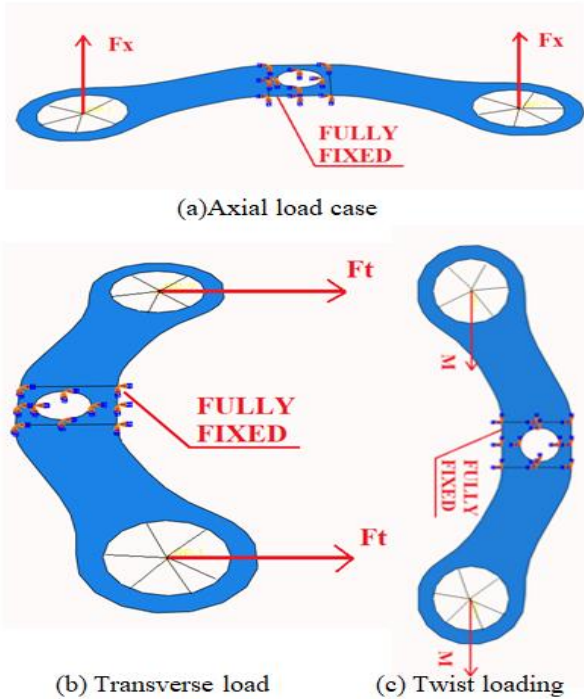


Fig. 8. Loading and boundary conditions for analysis

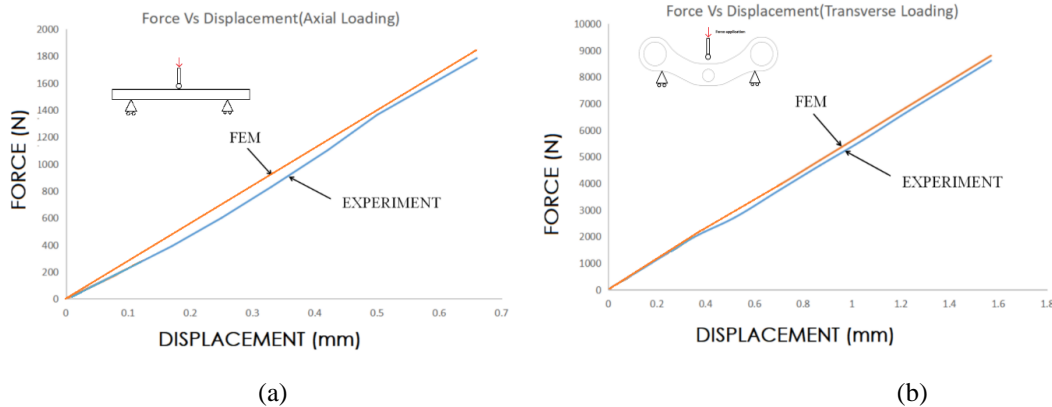


Fig. 9. Comparison of test and analysis results under (a) axial and (b) transverse loading for validation of FEM model. Similar result for the transverse loading is given in Fig. 9(b). The failure loads of the steel clamp based on von Mises criterion, are given in Table II. The stiffness values of steel clamp are given in Table III. Comparison of stiffness of steel and high modulus composite clamp for the new design (Table I) is also made in Table III. The deformed configuration of the composite clamp and the peak fiber stresses under the twist loading case are shown in Fig. 10.

**A. Comparison of Load-Displacement Variation (Low Modulus)**

The flexural modulus along longitudinal and transverse directions for the low modulus fabric is obtained from the present test as 8.4 GPa (all other mechanical properties are

constrained as shown Fig. 8(a).

**D. Type of Loading for Evaluation of Transverse Stiffness (High Modulus)**

Fig. 8(b) shows a typical load of 1000N at each end. Fully constrained boundary is given.

**E. Type of Loading for Evaluation of Twist Stiffness (High Modulus)**

Fig. 8(c) shows fully constrained boundary condition. A typical load of  $M=100$  N-m moment is applied to the loading nodes (Fig. 8(c)).

**VII. RESULTS AND DISCUSSION**

For the realized hardware of low modulus triple clamp, NDT has been carried out by coin tapping and visual inspection [8]. Minor edge delamination has been observed over a length of 20 mm between a few top layers. Hence three-point bend test is done with the debond area under compression.

Comparison of axial displacement (Fig. 6(c)) under three-point bend test and analysis for the low modulus composite triple clamp is shown in Fig. 9(a).

**B. Structural Characteristics of Steel Triple Clamp**

Based on the finite element analysis, the failure loads  $F_{xu}$ ,  $F_{tu}$  and ultimate moment,  $M_u$  (Eqn. (1)) are given in Table II. The stiffness  $K_x$ ,  $K_t$  and  $K_\theta$  of the steel clamp are given in Table III. Corresponding to the transverse failure load, the twist load from Eqn.

## Design of a High-Performance Composite Triple Clamp of Motorbike

(1) is estimated as 4400 N-m, which is much higher than the failure load of 350 N-m (Table II). In other words, the possible value of maximum transverse load is limited to 700 N (=  $M/0.5m$ ). Hence very high margin exists. The mass of the metallic clamp is 1.270 kg.

**Table- II: Failure loads of steel triple clamp**

Type of load	Failure load w.r.t strength 1185 MPa
Axial loading, $F_{xu}$	7990 N
Transverse loading, $F_{tu}$	8800 N
Twist loading, $M_u$	350 N-m

### C. Structural Characteristics of Steel Triple Clamp

Based on the finite element analysis, the failure loads  $F_{xu}$ ,  $F_{tu}$  and ultimate moment,  $M_u$  (Eqn. (1)) are given in Table II. The stiffness  $K_x$ ,  $K_t$  and  $K_\theta$  of the steel clamp is given in Table III. Corresponding to the transverse failure load, the twist load from Eqn. (1) is estimated as 4400 N-m, which is much higher than the failure load of 350 N-m. In other words,

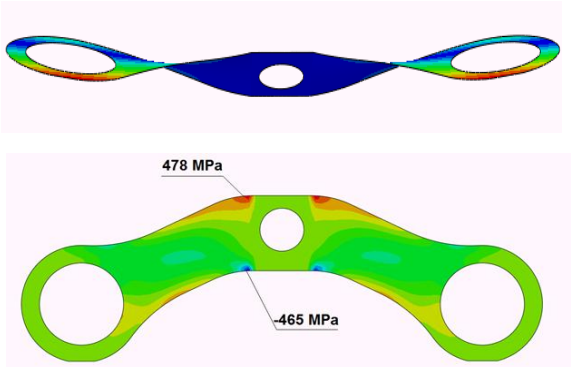


**Fig. 10. Deformed configuration and locations of maximum fiber stress in composite clamp under twist loading.**

the possible value of maximum transverse load is limited to 700 N (=  $M/0.5m$ ). Hence very high margin exists when compared to transverse load capability of 8800 N.

**Table- III: Comparison of stiffness of steel and high-performance composite clamp**

Stack-up sequence	Twist stiffness	Transverse stiffness
$(0_2/\pm 45)_{30S}$	418 N-m/deg	90.9 kN/mm
$(0_2/\pm 50)_{30S}$ (present design)	438 N-m/deg	90.9 kN/mm
$(0_2/\pm 55)_{30S}$	444 N-m/deg	83 kN/mm
$(0_2/\pm 60)_{30S}$	436 N-m/deg	77 kN/mm

### D. Design of High-Modulus Triple Clamp

A comparison of stiffness for the steel and composite clamp is made in Table III. Composite clamp mass is estimated as 270 gm. In the case of axial stiffness, the composite design shows an increase by 12% when compared to the steel clamp. The clamp shows a marginal increase in transverse stiffness with

similar twist stiffness value for both metallic and composite clamps. Fig. 10 shows the deformed configuration under twist load by 710  $\mu m$ . Corresponding to the twist failure load of the steel clamp (350 N-m), the present design shows a maximum fiber stresses of +478 MPa and -465 MPa as expected against its tensile strength of 1600 MPa and compressive strength value of 1000 MPa respectively (Fig. 10). A considerable margin against failure is observed for axial and transverse load cases (Table IV).

**Table- IV: Maximum fiber stress in composite clamp**

Load case	Maximum fiber tensile stress	Maximum fiber compressive stress
Axial	449 MPa	438 MPa
Transverse	319 MPa	232 MPa
Twist	478 MPa	465 MPa

It may be noted that the possibility for failure by delamination is not assessed. As a general practice in manufacturing of composite products, hoop windings of two or four layers are usually provided to avoid any possible delamination. In the present study also, two layers were provided over both arms of the clamp with an additional mass of about ten grams.

As mentioned in Sec. IV, the  $\alpha$  is arrived at 50 degrees (Fig. 5(b)). The twist and transverse stiffness at various values of  $\alpha$  are tabulated in Table V. From the table it is observed that as fiber angle  $\alpha$  varies from 45 to 60 degrees, twist stiffness reaches a maximum at around  $\alpha = 55^\circ$  and transverse stiffness reaches a peak value corresponding to the present design value of  $\alpha = 50^\circ$ . A minor increase of twist stiffness by 6% can be obtained for  $\alpha = 55^\circ$  plies. But for any new design with higher design specification, the proposed design methodology can be accepted as novel approach.

**Table- V: Stiffness variation with ply-orientation**

Performance characteristics	Steel design	High modulus composite clamp
Axial Stiffness, $K_x$	20.8 kN/mm	23.3 kN/mm
Transverse Stiffness, $K_t$	83.3 kN/mm	90.9 kN/mm
Twist Stiffness, $K_\theta$	449 N-m/deg	438 N-m/deg

## VIII. CONCLUSION

A design concept of a high performance composite triple clamp of a motorbike for 400 cc class has been established that satisfies both stiffness and strength criteria. A low modulus triple clamp has been fabricated and tested and the finite element model has been validated based on a good agreement on load –displacement behavior of the two approaches. High modulus carbon-epoxy laminate with proposed lay-up sequence has met the design adequacy. For the present design a 12% increase in axial stiffness with almost similar transverse and twist stiffnesses have been observed when compared to the steel triple clamp with an estimated mass reduction by 70%.

It has been concluded that corresponding to the critical load case of twist mode, the high-performance triple clamp possesses an expected margin of two.

The design methodology of the composite triple clamp for the selection of fibre angles for the lay-up sequences has been arrived at.

## REFERENCES

1. E. M. Odom and D. F. Adams, "Design and fabrication of a motorcycle swingarm utilizing composite materials", (No. 820990), SAE Technical Paper, 1982.
2. E. Dragoni and F. Fabio, "Design of a single-sided composite swing arm for racing motorcycles." *International Journal of Materials and Product Technology*, vol. 13(3), 1998, pp. 411–420.
3. A. Airoidi, S. Bertoli, L. Lanzi, M. Sirna and G. Sala, "Design of a motorcycle composite swing-arm by means of multi-objective optimization", *Applied Composite Materials*, vol. 19(3), 2012, pp. 599–618.
4. Technical specifications of Dominar 400. <https://www.bajajauto.com/motor-bikes/dominar-400/specifications>, last accessed 2019/07/21.
5. G. E. Dieter, "ASM Handbook", ASM International, vol. 20-Materials Selection and Design.
6. S. Jose, R. R. Kumar, G. V. Rao and P. Sriram "Studies on mixed mode interlaminar fracture toughness of M55J/M18 carbon epoxy laminate", *Advanced composite letters*, vol. 9(5), 2000, pp. 335–340.
7. W. C. Young, R. G. Budynas, A. M. Sadegh, "Roark's formulas for stress and strain", vol. 7, New York: McGraw-Hill, 2002.
8. S. D. Kim, C. W. In, K. E. Cronin, H. Sohn and K. Harries, "Reference-free NDT technique for debonding detection in CFRP-strengthened RC structures", *Journal of Structural Engineering*, vol. 133(8), 2007, pp. 1080–1091.

## AUTHORS PROFILE



equipment.

**Akshay B**, is a graduate in Mechanical Engineering from College of Engineering Trivandrum (affiliated to APJ Abdul Kalam Technological University) in 2019. His field of interest is composite design, machine design and structural analysis. He has some practical experience by working with the industries in designing automation



analysis of structures, computational fluid dynamics and CAD.

**Sony Alias**, is a graduate in Mechanical Engineering from College of Engineering Trivandrum (affiliated to APJ Abdul Kalam Technological University) in 2019. His final year project work was on the "Design and Analysis of a High-Performance Composite Triple Clamp of Motorbike". His field of interest covers design and



More details on CV is available in

<https://orcid.org/0000-0001-5640-2066>.

**Dr. R. Ramesh Kumar**, is currently working as a Nodal Research Officer and Professor in Sree Chitra Thirunal College of Engineering, Thiruvananthapuram, Kerala, India, since July, 2014. Prior to that served in Vikram Sarabhai Space Centre, ISRO, India for about thirty

years. Fields of interest include, Design / analysis of composite structures for launch vehicles, Thermo-structural analysis of nozzles, Buckling of sandwich structures, Analytical approach for reinforced holes in shells etc.